The importance of wind as a driver of earthen heritage deterioration in dryland environments

J Richards[1*], H Viles[1], Q Guo[2]

[1] Oxford Resilient Buildings and Landscapes Lab, School of Geography and the Environment, University of Oxford, Oxford OX1 3QY, UK

[2] Dunhuang Academy, Dunhuang, 736200, China

*corresponding author: Jennifer.richards@ouce.ox.ac.uk

Highlights

- Geomorphological signatures reveal drivers of earthen heritage deterioration
- High frequency of wind events in drylands causes substantive cumulative impact
- Wind-driven deterioration features typically have low persistence
- Wind is an important initiator of earthen heritage deterioration

Abstract

Dryland regions are exposed to extreme environmental conditions that create hotspots of weathering and erosion. Many earthen heritage sites are located in these dryland regions and experience extensive deterioration driven by interactions with environmental processes, however previous research has focused largely on the role of rain as a driver of deterioration. This study combines approaches from geomorphology with understandings of earthen materials from heritage science to investigate the relative importance of wind and rain in driving earthen heritage deterioration in drylands. We use geomorphological signatures to infer the environmental histories of earthen walls with a range of known ages at Suoyang Ancient City, China, using semi-quantitative deterioration assessments. We find rain-driven deterioration features to be associated with the loss of larger volumes of material and to have higher persistence than wind-driven deterioration features. However, we argue that the high frequency nature of wind events means that wind is an

important initiator of deterioration across the site. In addition, walls exposed to the prevailing wind are dominated by wind-driven deterioration features. Outcomes from this study present an opportunity for earthen heritage conservation to investigate potential strategies to minimise wind speed at earthen heritage sites in drylands.

Key Words: earthen heritage, deterioration, frequency, magnitude

1 Introduction

In dryland regions, extreme environmental conditions can cause hotspots of weathering and erosion to occur (Xie et al., 2007; Viles and Goudie, 2007, 2013; Shao et al., 2013). Strong winds can remove material through deflation and abrasion (Wang et al., 2010; Mao et al., 2015), while sporadic rainfall events can erode material through processes such as splash, rill, gully and sheet erosion (Luo et al., 2019; Beckett et al., 2020). There is a long history of research on the impact of environmental drivers on in-situ rock breakdown in drylands (Loughlin, 1931; Schaffer, 1932; Huinink et al., 2004; Momeni et al., 2015) and the evolution of landforms such as yardangs (Ward and Greeley, 1984; Goudie et al., 1999; Li et al., 2016; Pelletier et al., 2018). However, notably less research has investigated the impact of environmental drivers on building materials used in dryland regions.

Understanding the drivers of deterioration for earthen building materials in dryland regions is highly important as, due to the widespread availability of earth as a building material, many earthen heritage sites are found there (WHEAP, 2012). The value of many earthen sites is linked to the presence of authentic materials (Richards et al., 2018), but these materials are currently experiencing extensive deterioration (Xie et al., 2007; Wang et al., 2010; Shao et al., 2013; Pu et al., 2016; Richards et al., 2020). Earthen materials have been found to have a low durability to environmental processes (Beckett et al., 2020). For example, rain and wind-driven rain (hereafter both referred to as rain) can weaken cementing material between particles, caused by dissolution and hydration reactions of key compounds (Shao et al., 2013; Richards et al., 2019). Clean wind can deflate loose earthen material (Richards et al., 2019). If the wind is sediment laden, the impact of airborne particles hitting the earthen material can cause grains of earthen material to be loosened or to break off from the parent material resulting in abrasion (Wang et al., 2010; Mao et al., 2008, 2015; Richards et al., 2019). Without the development of conservation strategies that effectively reduce rates of material loss at these sites, further damage to earthen heritage sites is inevitable. Consequently, there is an urgent need to understand the relationships between environmental

54 processes and earthen heritage deterioration. In particular, we need to understand: (i) the nature
55 and distribution of environmental drivers of deterioration, (ii) the frequency and magnitude at which
56 each driver occurs and (iii) the persistence of resultant deterioration features.

57 Earthen heritage research has predominantly focused on identifying drivers of deterioration but has
58 not yet addressed the relative extent to which these drivers cause the loss of historic material (Shao
59 et al., 2013; Pu et al., 2016; Du et al., 2017). This lack of research is caused, in part, by limitations in
60 many experimental setups, with experiments investigating the impact of single environmental
61 drivers in isolation from other drivers (Luo et al., 2019); not being run for long enough to allow
62 deterioration features that form at slower rates to develop (Pu et al., 2016; Richards et al., 2019);
63 not capturing the complexity of on-site conditions (Mao et al., 2015); and overlooking the important
64 differences in the magnitude and frequency of events (Bruno et al., 1968). Similar methodological
65 challenges have also been faced in geomorphology. In response to these challenges,
66 geomorphologists have used geomorphological signatures (the palimpsest of weathering or
67 erosional features present on a given surface area) to infer environmental histories over a range of
68 scales from sand grains to boulders to landscapes (Lancaster, 1995; Viles, 2001; Bourke et al., 2007;
69 Ehlmann et al., 2008).

70 In this paper, we apply approaches used in geomorphology, which assess impacts of weathering and
71 erosion on rock and soil surfaces, and apply them to earthen heritage. We use geomorphological
72 signatures as a method to investigate the relative importance of environmental drivers of
73 deterioration on earthen walls with a range of known ages. In particular, this study addresses the
74 following questions:

75 i) To what extent do wind and rain drive deterioration processes on earthen heritage in
76 arid and semi-arid areas?
77 ii) How should understanding of these interactions inform conservation strategies for
78 earthen heritage?

Earthen heritage is constructed from a range of materials that each have unique interactions with environmental drivers of deterioration (e.g. adobe, rammed earth, cob). To reduce complexity, this study focuses on heritage sites constructed of rammed earth. This is justified as: (i) many earthen sites in dryland regions are constructed of rammed earth; (ii) many rammed earth sites are experiencing widespread deterioration; and (iii) rammed earth has been understudied in comparison to other earthen materials such as adobe (e.g. Brown et al., 1979; Selwitz et al., 1990; Taylor, 1990; Oliver et al., 2000; Guerrero, 2002; Illampas et al., 2013).

Rammed earth is constructed by compacting layers of raw earth within a temporary frame to create a compacted, solid material. Historically compaction was undertaken using a ramming tool resulting in a distinctive layering pattern. Once the desired height of the wall was reached, the frame was moved along and the process repeated to create a continuous wall. In particular, this paper focuses on the understudied and remote site of Suoyang Ancient City, one of over 400 earthen sites located in northwest China, many of which are experiencing extensive deterioration (Mao et al., 2015).

2 Material and methods

2.1 Study site: Suoyang Ancient City

Suoyang Ancient City (锁阳城), hereafter known as Suoyang, is located in Gansu Province, north west China, on the ancient Silk Road. It is an archaeological site built from rammed earth during the Han (206 BCE–220 CE) and Tang (618 – 907 CE) dynasties and abandoned ~400 years ago (Xie et al., 2007). The site covers over 1 km^2 and consists of inner city walls (approximately 500 m^2; Figure 1a), outer city walls, a monastery (Figure 1b), animal enclosures, archery platforms and an extensive irrigation system (UNESCO, 2014). In 2014, Suoyang was enlisted as one of 33 sites that form the Silk Roads World Heritage Site. The site exhibits a variety of deterioration features such as polishing, pitting, slurries and scouring as well as formation of cracks, gullies, slumps and collapses (Richards et

Deleted:

Deleted:

al., 2019), which have similarities with weathering and erosional features found on rock walls (Messenzehl et al., 2018), cliff faces (Kuenen, 1948) and earthen hillslopes (Xu et al., 2017).

The site has a continental semi-arid climate with temperatures exceeding 35 ^{o}C in summer and falling below -30 ^{o}C in winter (UNESCO, 2014). According to the Köppen-Geiger climate classification, Suoyang is located in an area classified as 'BWk', indicating that it is in an arid desert environment where the mean annual temperature is less than 18^{o}C (Peel et al., 2007). Precipitation is seasonal with most falling during spring and summer. Between 1986 and 2005, the average annual precipitation was 49 mm but ranged from 33 to 74 mm with the maximum single rainfall event recorded at 30 mm. Wind speed and direction is highly seasonal with strong easterlies occurring in the summer months (Dunhuang Academy, unpublished).

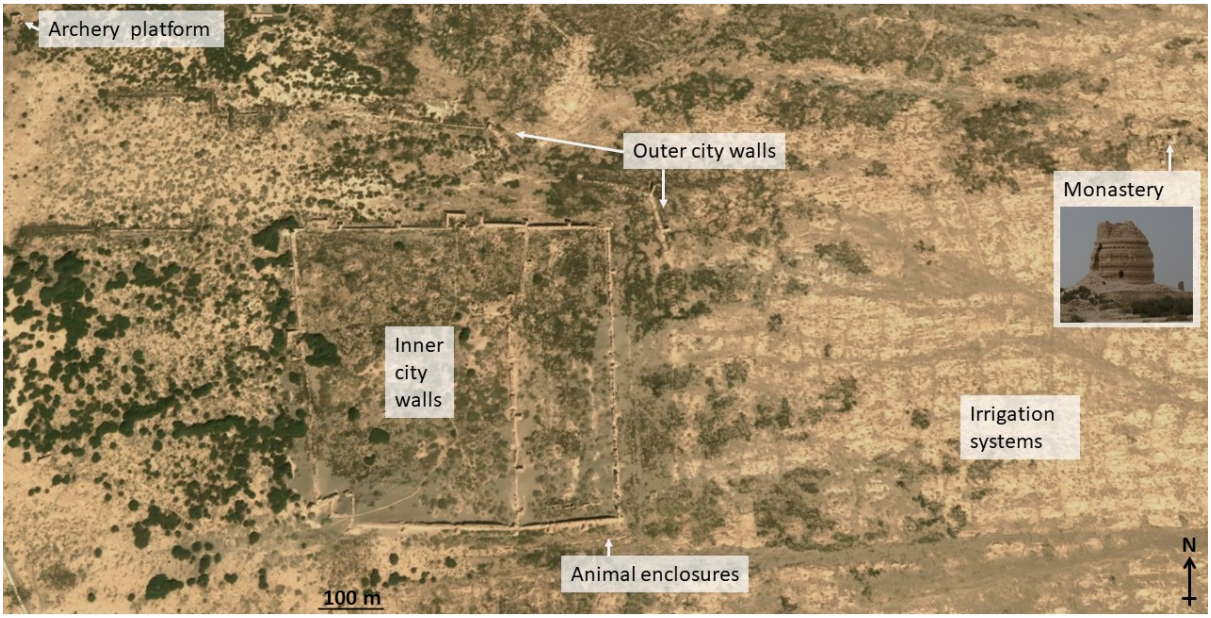

Figure 1: An aerial view of Suoyang Ancient City showing the location of the inner and outer city walls, one of the archery platforms, animal enclosures, irrigation systems and monastery (photo inset: author's photo). Photo credit: Google Earth.

Suoyang's remote location and harsh climate have precluded much scientific research. However, since 2015, Dunhuang Academy have established an experimental test area to the east of the main site. Two sets of test walls (large and small) have been built in this experimental area, allowing a

range of tests to be undertaken on and around earthen walls without harming the historic material. As such, Suoyang provides a unique opportunity for the investigation of environmental and deteriorative processes to be studied at a remote earthen site, which has many similarities to other earthen sites in this area.

2.1.1 Experimental area: Test walls

Both sets of test walls in the experimental area were used in this study. The set of small test walls was built in April 2015. We used the wall from the set that was built to replicate the material properties of the historic walls at Suoyang (Figure 2). This small test wall faces north and was built against a yardang using loessic soil taken from areas around Suoyang, with similar particle size distribution to the historic material. The wall was constructed using traditional ramming techniques as described above. The wall is formed of six layers and measures 64 cm high and 76 cm wide, with a dry density of 1.70 g cm^{-3}. The wall has been exposed to the environment for three years and is now assumed to be in equilibrium with environmental conditions. For more information see Richards et al. (2019).

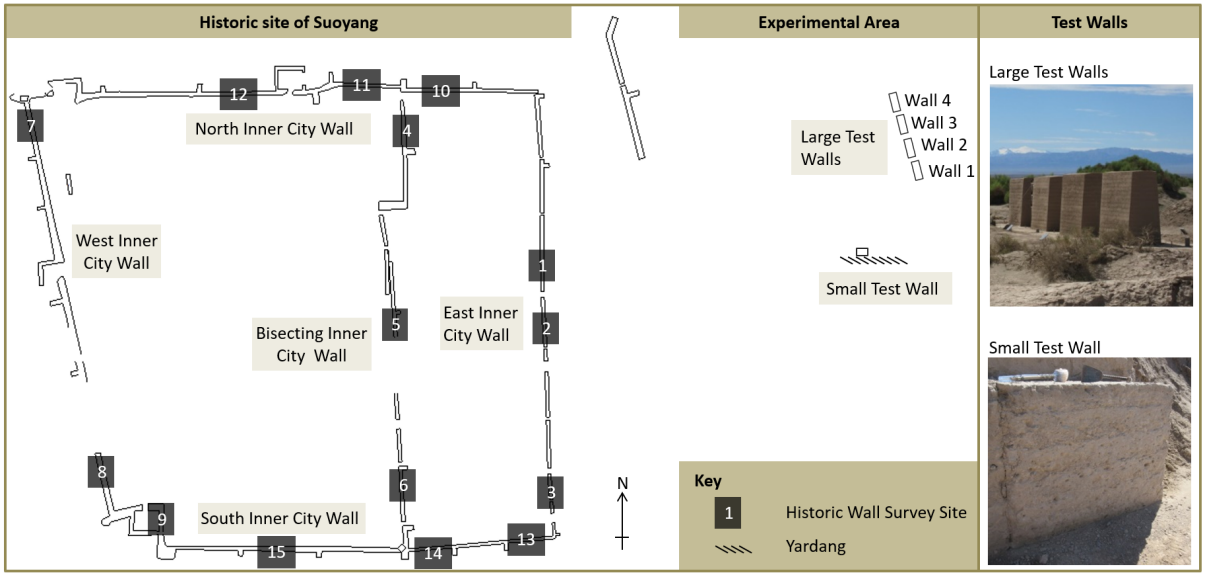

Figure 2: A plan view of Suoyang showing the location of the small test wall, large test walls and inner city walls. Sites for expert deterioration survey assessment on the inner city walls are indicated.

Four large test walls (210 x 300 x 100 cm) were also built by Dunhuang Academy in July 2017, perpendicular to the prevailing easterly wind. These walls were constructed in a similar manner to the small test wall with two different dry densities representing a deteriorated (1.65 g cm^{-3} – Wall 1 and 2) and non-deteriorated state (1.75 g cm^{-3}- Wall 3 and 4; Figure 2). These walls have been exposed to the environment for more than a year and are also assumed to be in equilibrium with the environment.

Deleted:

Fieldwork was undertaken in August 2018 as part of a wider project investigating potential conservation methods for Suoyang. Data collection focused on a range of locations on the historic inner city walls and on the test walls in the experimental area (Figure 2). During the fieldwork, on the 14^{th} – 15^{th} August, a 36-hour storm occurred with strong westerly winds gusting over 17 ms^{-1} and heavy rain.

Deleted:

2.2 Approach

In this study, we assessed the relative importance of wind and rain as drivers of deterioration by using semi-quantitative visual methods to characterise the type and severity of deterioration features associated with wind and rain present on the wall face (Mottershead, 2000; Wright, 2002). Together these features formed a geomorphological signature that was used to infer the deterioration history of Suoyang (Figure 3) (Ehlmann et al., 2008).

Deleted:

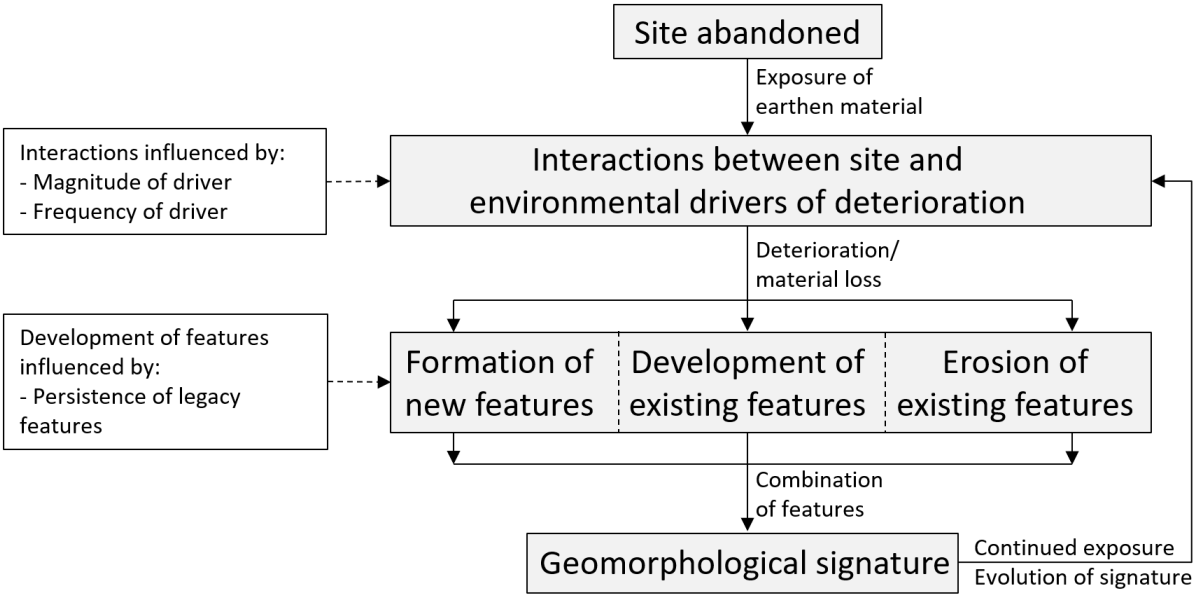

182

183 **Figure 3: Our approach for assessing geomorphological signatures through the formation of deterioration features**

184 Research suggests that geomorphological signatures are likely to be influenced by: (i) the frequency
185 and magnitude of environmental drivers (Brunsden and Thornes, 1979; Goudie and Viles, 1999;
186 McKay et al., 2009), and (ii) the persistence of deterioration features in the face of subsequent
187 events, where persistence refers to the duration of time a deterioration feature remains visible after
188 its formation (Figure 3) (Bourke et al., 2008). However, in the earthen heritage literature, there has
189 been little discussion of these concepts.

Deleted:

190 To assess geomorphological signatures on earthen heritage, we surveyed deterioration features
191 present on test and historic walls that had been exposed to deteriorative environmental conditions
192 for different lengths of time. At all survey sites, deterioration features were identified using a key
193 developed by the authors using information collected from a preliminary visit to the site in August
194 2017 (Table 1). The severity of identified features was ranked on a four-point scale with respect to
195 the feature's spatial coverage: absent (-), present in a localised area (*), present in multiple areas
196 (**) or extensive coverage (***).

Deleted:

197 We used abductive reasoning to determine the environmental process(es) likely to have caused the
198 deterioration features. This reasoning was informed by literature (see Table 1) and the authors'

Deleted:

previous experimental work and experience (e.g. Richards et al., 2019) to minimise any potential issues caused by equifinality.

204 **Table 1: Descriptions and the inferred causes of deterioration features at Suoyang.**

Deterioration feature	Description	Inferred Cause	Literature
Wind-polishing	Surface smooth with all loose material removed. No grooves or scouring marks.	Clean wind	Lancaster (1984) Shao et al. (2013)
Sand-polishing	Surface smooth with all loose material removed. Thin scouring lines are present. Lines are normally horizontal or in the direction of the wind flow around the wall.	Sediment laden wind	Laity (2009) Laity (2011)
Rounded corners	Corners and edges of walls (both vertical and on the wall top) are rounded with no distinct sharp edge.	Clean wind Sediment laden wind	Fujii et al. (2009)
Scouring at base	Distinct grooved lines at the base of the wall in the direction of the wind flow around the walls. Grooved lines are generally thicker than those found higher up the wall. Some scouring material may also be present.	Sediment laden wind Fast clean winds	
Pitting/hollowing	Removal of material from a localised area. The surface is normally rough and concave.	Sediment laden wind Fast clean winds	Shao et al. (2013)
Flaking	Thin surface layer of material detached from main body of wall and peeling off in flakes.	Wind-driven rain Vertical rain	Bruno et al. (1968) Cui et al. (2019)
Slurry	Crust on wall surface formed down the wall face. Generally smooth surface.	Wind-driven rain Vertical rain	Crosby (1983) Shao et al. (2013)
Gully	Vertical indent or gorge into the wall surface. Normally occurs below a nook or low point in the wall height.	Vertical rain Wind-driven rain	Bruno et al. (1968) Du et al. (2017)
Outwash slope	Sediment at the base of the wall fanning away from the wall. Usually poorly sorted with consolidated lumps of earthen heritage present.	Wind-driven rain Vertical rain	
Turreting and wall collapse	Substantial or complete loss of material from wall causing stepped changes in wall height.	Wind-driven rain Clean wind Sediment laden wind	Bruno et al. (1968)

205

2.2.1 Assessment of geomorphologic signatures on small test wall

On the small test wall, field experiments were run to produce geomorphic signatures under controlled experimental conditions. The wall was cleaned to remove any naturally occurring deterioration features already present and then exposed to clean wind, sediment laden wind and rain representative of conditions experienced at the site over a period of days to months (Richards et al., 2019). The wall was scanned using a handheld Creaform Handy SCAN 700 3D™ laser scanner (0.2 mm accuracy, 0.050 mm resolution) before and after each experimental run. The surface spatial grid data was analysed using Geomagic Control, with the point cloud being processed into a 3D mesh. Pre- and post-test meshes were aligned and the topography compared to identify any changes to the wall surface (Barton, 2009). Any changes to the wall surface were then assessed using the deterioration key (Table 1) and the extent of the deterioration features ranked. For more information on the experimental setup see Richards et al. (2019).

2.2.2 Assessment of geomorphologic signatures on large test walls

At the time fieldwork was undertaken, the large test walls had been exposed to environmental processes for approximately 1 year. Visual assessments were undertaken on each vertical face of the test wall and analysed for notable deterioration features (Rothert et al., 2007) using the deterioration key (Table 1).

2.2.3 Assessment of geomorphologic signatures on historic inner city walls

The historic inner city walls have been exposed to environmental processes over several centuries, having been constructed over a millennium ago and abandoned approximately 400 years ago (UNESCO, 2014). To assess the variability in deterioration features on the historic walls, the inner city walls were divided into five wall sections: north, south, east, west and bisecting (central). Three sites on each wall section were selected using a combination of systematic and opportunistic sampling to ensure that, where possible, the full length of each wall was surveyed (Figure 2 – sample

Deleted:

Deleted:

Deleted:

sites are numbered 1 to 15). At each survey site, vertical wall faces were assessed for deterioration features (Table 1).

3 Results

3.1 Small test wall

After the field experiment, geomorphological signatures on the small test wall were composed of a limited number of deterioration features (one to three) at an early stage of formation (Table 2). Clean wind caused small amounts of loose material to be removed from protruding areas resulting in polishing (Figure 4a). Sediment laden wind caused loose material to be removed from the surface, as well as the abrasion of small grains of material, resulting in incipient pitting (Figure 4b). Rain caused soil particles to be entrained and transported down the wall face resulting in incipient gullying (Figure 4c). The severity of the deterioration features varied, with the clean wind causing minimal, localised impacts while the sediment laden wind and rain caused more extensive deterioration.

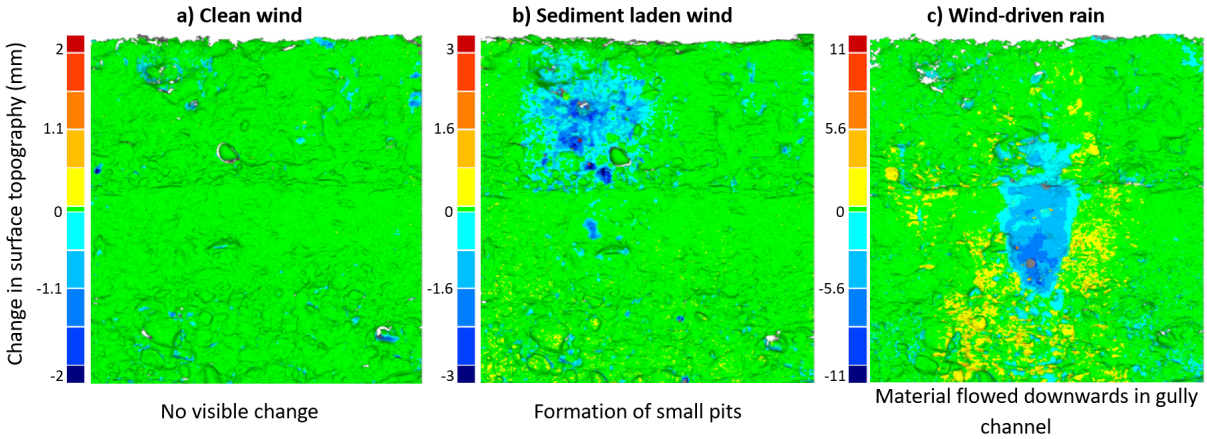

Figure 4: Deviation maps showing change in surface topography (mm) after being exposed to a) wind, b) sediment laden wind and c) rain. Note the different scales for each deviation map. Adapted from Richards et al., (2019).

253 **Table 2: The types and severity of deterioration features present on the small test wall, large test walls and inner city**

254 **walls**

			Wind					Rain				Both
Aspect	**Location/sample site**		**Wind-polishing**	**Sand-polishing**	**Rounded corners**	**Scouring at base**	**Pitting/ hollowing**	**Flaking**	**Gully**	**Slurry**	**Outwash slope**	**Turretting**
N/A	Small test wall: Wind		*	-	-	-	-	-	-	-	-	-
	Small test wall: Sediment laden wind		*	*	-	-	**	-	-	-	-	-
	Small test wall: Rain		-	-	-	-	-	-	**	-	-	-
East	Large test wall 1		*	-	*	*	-	**	-	-	-	-
	Large test wall 2		*	-	*	*	-	**	-	-	-	-
	Large test wall 3		-	-	*	*	-	*	-	-	-	-
	Large test wall 4		-	-	*	*	-	*	-	-	-	-
West	Large test wall 1		-	-	*	-	-	***	-	-	*	-
	Large test wall 2		-	-	*	-	-	***	-	-	*	-
	Large test wall 3		-	-	*	-	-	***	-	-	*	-
	Large test wall 4		-	-	*	-	-	***	-	-	*	-
East	East inner city wall	Site 1	**	*	***	***	***	-	*	*	*	***
		Site 2	*	*	**	**	**	-	-	*	**	***
		Site 3	**	**	**	**	**	-	*	*	*	***
	Bisecting inner city wall	Site 4	**	***	**	-	*	-	*	**	**	-
		Site 5	**	***	**	*	*	-	-	*	**	**
		Site 6	*	***	***	-	**	*	-	**	**	*
	West inner city wall	Site 7	**	**	**	-	**	-	*	**	-	-
		Site 8	**	***	***	*	**	-	-	**	*	-
		Site 9	**	***	**	-	***	-	*	*	-	-
West	East inner city wall	Site 1	-	-	*	*	-	*	-	***	-	***
		Site 2	-	-	*	*	-	**	-	***	**	***
		Site 3	-	-	*	*	-	-	**	***	*	***
	Bisecting inner city wall	Site 4	-	-	*	-	-	**	-	***	***	-
		Site 5	-	-	*	-	-	*	-	***	***	**
		Site 6	-	-	*	-	-	***	-	***	***	*
	West inner city wall	Site 7	-	-	-	-	*	**	-	***	*	-
		Site 8	-	-	**	-	-	**	*	***	-	-
		Site 9	-	*	*	-	-	*	-	**	-	-
Internal	North inner city wall	Site 10	*	**	***	-	**	-	**	**	**	-
		Site 11	*	**	***	-	-	**	*	***	***	-
		Site 12	-	-	**	-	*	*	-	**	***	-
	South inner city wall	Site 13	**	***	**	-	**	*	*	**	**	-
		Site 14	*	***	**	-	***	-	*	**	**	-
		Site 15	*	**	**	*	**	**	-	***	***	-
External	North inner city wall	Site 10	*	***	*	-	**	-	*	**	**	-
		Site 11	**	***	*	-	**	-	-	***	**	-
		Site 12	**	***	**	-	**	*	-	***	*	-
	South inner city wall	Site 13	*	**	*	-	***	-	*	**	**	-
		Site 14	*	*	**	-	**	*	*	**	**	-
		Site 15	***	***	**	*	**	-	*	**	*	-

Key

-	absent
*	present in a localised area
**	present in multiple areas
***	extensive coverage

3.2 Large test walls

After exposure for 1 year, the geomorphological signatures on the large test wall each comprised three to four deterioration features associated with both wind and rain events (Table 2). All four test walls exhibited features including a slight rounding of corners and scouring around the base of the walls in an east-west direction (Figure 5a and b). On the western side, flaking was present across the entire wall face. On the eastern side there was variation in the deterioration features present across the wall face. On the two lower density walls (Walls 1 and 2), there was a notable change in the extent of flaking with height. On Wall 1, there was extensive flaking at the base of the wall to around 50 cm above the ground (Figure 5c). On Wall 2, there was minimal erosion at the base of the wall, with flaking only occurring around 1.75 m from the ground. This lack of flaking below 1.75 m is likely to be associated with the presence of a yardang to the east of the wall, approximately 1.5 m high, blocking the strong easterly winds from interacting with the base of Wall 2. On the two higher density walls (Walls 3 and 4) there was some less severe, patchy flaking occurring on the eastern side.

Development of deterioration features in real time was observed on the large test walls during the storm event on 14-15th August 2018. The storm caused a notable volume of material, comprised of a range of grain sizes, to be deposited at the base of the walls forming a small outwash slope. This was especially visible on the west side, facing the prevailing storm direction, where the deposited material extended outwards for almost 50 cm in some areas (Figure 5d).

Deleted:

Deleted:

Deleted:

Deleted:

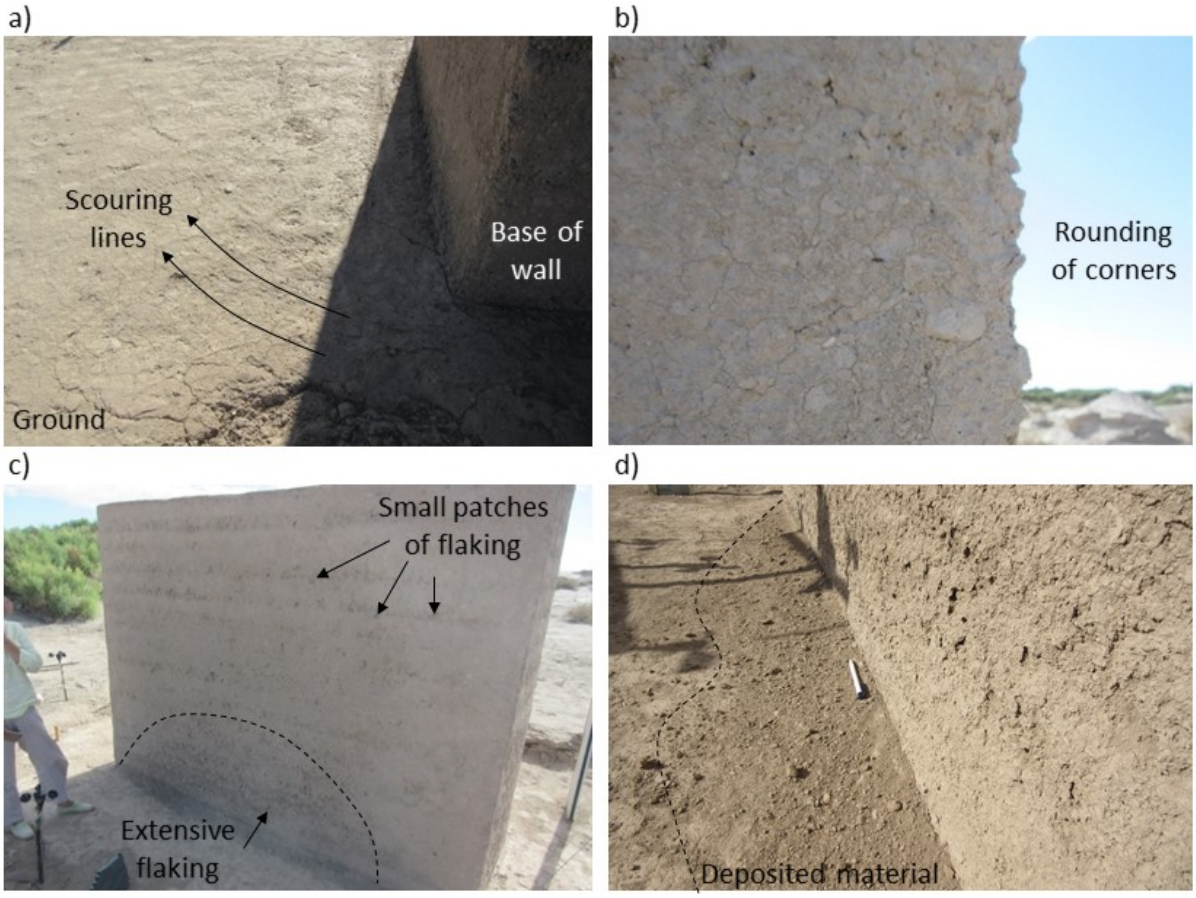

Figure 5: Deterioration features found on the large test walls after one year exposed to the environment at Suoyang: a) scouring around the base of the test walls, b) the rounding of the test wall corners, c) the variation in flaking on the eastern side of Wall 1 and d) The deposited material at the base of the west side of Wall 1.

3.3 Historic walls

The greatest variety in deterioration features was found on the historic walls with each signature comprising five to eight deterioration features associated with both wind and rain events (Table 2). The variability of deterioration around the site was also captured with the geomorphological signature varying significantly between different sections of the inner city wall and also within individual sample sites (Figure 6).

Deleted:

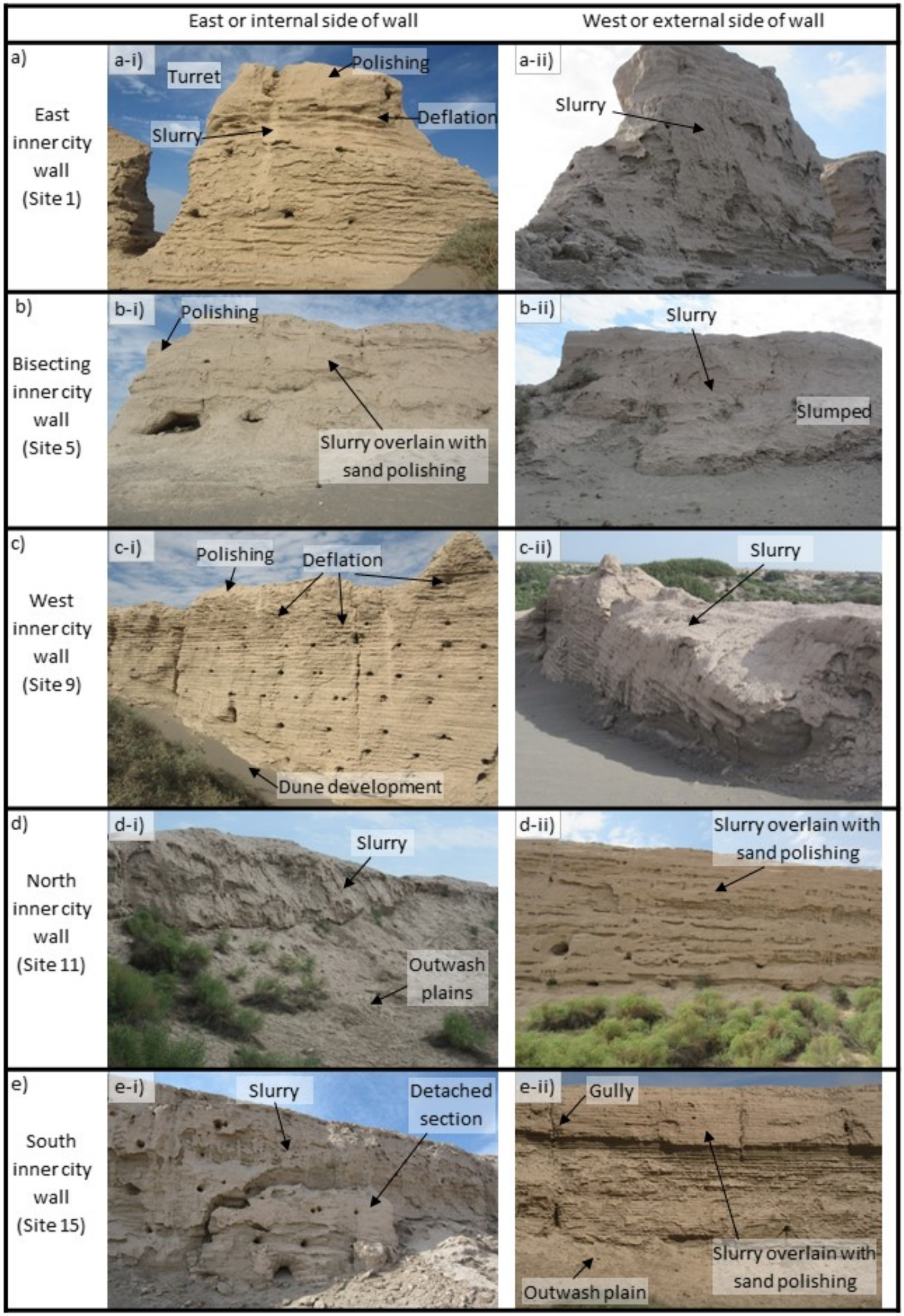

289
290 **Figure 6: Deterioration around Suoyang at the a) East, b) Bisecting, c) West, d) North and e) South inner city wall.**

291 **Deterioration on the east or internal wall face is shown in (i) and west or external wall face is shown in (ii).**

East inner city wall

The east inner city wall was degraded into turret shaped sections with some sections becoming free standing (Table 2). On the east side of the east inner city wall there was extensive hollowing and deflation with rammed earth layers clearly visible across the majority of the wall face (Figure 6a-i). At the base of the walls there was also extensive scouring and rounding of corners, especially on faces between wall sections. At the top of the walls there were notable patches of wind polishing and some small sections of slurry. The slurry tended to be located under small faults in the wall top and in some cases formed narrow gullies down the wall face. At the base of the wall there tended to be a small outwash plain.

On the west side of the east inner city wall, slurry covered almost all areas with multiple layers being visible on some wall sections (Figure 6a-ii). Gullies were also present and were deeper than on the east side of the same wall section. At the base of the wall, slurry had been undercut especially on wall sections which had a dune forming against the wall.

Bisecting inner city wall

The bisecting inner city wall was taller and the wall sections were more continuous (less turret-like) with fewer collapses than the east inner city wall (Table 2). On the east side of the bisecting inner city wall, extensive wind and sand polishing and rounded corners was present (Figure 6b-i). In addition, there were areas of slurry, some of which was overlaid with sand polishing. In areas where slurry had been eroded, either by under cutting or flaking off, material had been deflated. Gullies were present on some areas of the wall, predominately forming where cracks were present in the wall. The west side of the bisecting wall was notably more slumped with large dunes abutting the wall (Figure 6b-ii). There was extensive slurry across the wall surface and large outwash plains at the base.

West inner city wall

The west inner city wall was almost continuous. On the east side, wind and sand polishing, rounding of corners and deflation of material with some slurry and gullying were present at the north and south end, and there was extensive dune development almost burying the walls in some places in the centre (Table 2; Figure 6c-i). On the west side there was extensive dune development towards the centre of the wall. The exposed areas at the north and south end of the wall exhibited large amounts of slurry over the walls, deep gullies running down the wall face and out wash plains at the base of the walls (Figure 6c-ii).

North inner city wall

The north inner city wall was continuous (Figure 6d). The internal wall had extensive slurry coverage in some areas with large outwash plains at the base of the wall (Table 2; Figure 6d-i). Corners along the wall were rounded but there was variation in the extent to which there was deflation, dune development and gullying on the walls. Some areas showed a palimpsest of deterioration features with sand polishing overlaying slurry.

The deterioration features along the external wall were similar except for around the fortification towers where slurry was more dominant on the leeside of the towers. On all other areas, there was a thin slurry down the walls with sand polishing on top and shallow gullies down the wall with outwash fans at the base (Figure 6d-ii).

South inner city wall

The south inner city wall also was also continuous. However, parts of the internal wall showed evidence of collapse and had thick slurry occurring along the entire length with shallow outwash plains along the base of the wall (Table 2). Over the top of the crust, there was notable horizontal wind polishing (Figure 6e-i). In addition, deep gullies were present with outwash fans at the base of the gully. The deterioration features on the external wall were similar to those found on the external

north inner city wall: in all areas except for around fortification towers there was thin slurry overlaid with sand polishing (Figure 6e-ii).

4 Discussion

We used geomorphological signatures present on the test and historic walls at Suoyang to investigate the relative importance of wind and rain as drivers of earthen heritage deterioration. By combining the geomorphological signature data from the test and historic walls (Table 2, Figure 4 - Figure 6), Table 3 ranks the relative importance of wind- and rain-driven deterioration features over different exposure periods using a five-point scale. This type of classification scale has recently been used by Du et al. (2020) to undertake damage assessments of collapses along the Ming Great Wall, China. Given the ability of this method to compare the extent of deterioration with characteristics of specific deterioration features, in this study we use a similar scale to assess the relative importance of wind- and rain-driven deterioration features with regard to:

(i) the nature and distribution of features.

Volume: A value of '1' was assigned to features formed with the erosion/ deposition of small (cm^3) quantities of sediment off the wall surface, while '5' was assigned to features formed with the erosion/ deposition of large (m^3) quantities of sediment that threaten the structurally integrity of the wall.

Spatial coverage: A value of '1' indicated a presence on in localised areas, while '5' indicated a complete, widespread presence across the wall face.

(ii) the frequency and magnitude of deteriorative events required to drive a feature's formation.

Number of events: A value of '1' was assigned to features that formed after exposure to many deterioration events (100s), while '5' was assigned to features formed within a single deterioration event.

Time to formation: As deterioration events in dryland regions occur at different

frequencies, deterioration features that form over long temporal periods (decades) were assigned a '1'. Features that form over short temporal periods (days) were assigned a '5'.

(iii) the persistence of a feature to future deteriorative events.

Persistence: A value of '1' was assigned to features erased by subsequent deterioration events. '5' was assigned to features still present after numerous (100s) subsequent deterioration events.

Table 3: Comparing the nature and distribution, frequency and magnitude and persistence of wind- and rain-driven deterioration features on earthen heritage

		Wind-driven features					Rain-driven features				Both
		Rounded corners	Scouring at base	Sand polishing	Wind polishing	Pitting	Flaking	Slurry	Gully	Outwash slope	Turretting
Nature and distribution	Volume of material eroded or deposited during feature formation (1=small, 5=large)	1	1	1	1	2	2	3	4	4	5
	Spatial coverage of feature at Suoyang (1=localised, 5=widespread)	1	1	2	3	4	3	4	1	3	2
Frequency and Magnitude	Number of wind/rain events for feature to form (1=many events, 5=few events)	3	3	1	1	1	3	3	4	4	1
	Time period for feature to form in semi-arid regions (1=long period, 5=short period)	5	5	3	3	4	4	2	2	3	1
Persistence	Persistence of feature to wind events (1=low, 5=high)	-	-	-	-	-	3	4	4	3	5
	Persistence of feature to rain events (1=low, 5=high)	1	1	1	1	1	-	-	-	-	5

4.1 Nature and distribution of deterioration

In this study, we found substantive differences in the nature of deterioration features caused by wind and rain in terms of volume of material moved and spatial coverage (Table 3). As found experimentally on the small test wall, wind generally removed less material per event than rain

Deleted:

(Figure 4). Similarly, on the historic and large test walls, wind-driven deterioration features were commonly formed with the loss of small volumes of material while a greater amount of material typically moved to form rain-driven features (Figure 5 and 6). These results correspond well with previous research that has also found that features, such as polishing, are commonly formed on areas where individual loose grains have been deflated, while features such as gullies can transport large amounts of material en masse down the wall face (Wang et al., 2010; Mao et al., 2015; Richards et al., 2019, 2020).

Of the deterioration features assessed in this study, turretting was associated with the greatest material loss. It was only found on the historic walls (Table 2) suggesting that this feature develops over longer temporal periods and on larger structures than other features such as polishing or rounding of corners. The regular spacing of turrets along the east inner city wall further suggests that deterioration is focused on the joints between the constructed sections of rammed earth, although this process could also occur on areas where vertical cracking has developed due to the uneven settlement of foundations. Interactions and feedbacks in these joint areas between gullying and wind deflation processes seem to be vital in causing the development of fissures in the wall face (Du et al., 2017; Cui et al., 2019; Richards et al., 2020). However, the location of severe turretting on the eastern inner city wall, exposed to the prevailing wind, compared to the absence of turretting on any other inner city wall (Table 2), strongly implies that wind is likely to be the initiating factor in the formation of these large deterioration features.

Results from the test and historic walls show the distribution of other wind- and rain-driven deterioration features are constrained by spatial factors (Table 4). Both wind and rain features were seen to be controlled by the aspect of the wall, with prevailing climatic conditions strongly influencing the type of deterioration present on the historic and test walls. On both the test and historic walls, wall faces exposed to the prevailing wind direction tended to be dominated by wind-driven deterioration features, while wall faces exposed to the prevailing storm directions tended to

Deleted:

Deleted:

Deleted:

Deleted:

Deleted:

be dominated by rain-driven deterioration (Figure 5 and 6; Table 2). The presence of wind-driven deterioration features was also seen to be strongly dependent on the spatial location across the wall face with respect to: the vertical height of the wall, the edge of the wall and the location of the saltation zone up the wall face (Table 4; Richards et al., 2020). The presence of rain-driven deterioration features is notably dependent on the location of cracks or joins in the earthen material (see Table 4 for further detail).

Table 4: Spatial controls on a) both wind- and rain-driven deterioration features, b) wind-driven deterioration features and c) rain-driven deterioration features.

Spatial control	Reason	Impact
a) Wind and rain		
Aspect	The prevailing wind is easterly while the prevailing direction of storms is westerly	The presence of wind-driven deterioration features is dominant on the east wall faces while rain-driven deterioration features are dominant on the west wall faces
b) Wind		
Vertical height	Wind velocity increases with height from the ground	Presence of features formed by the deflation of loose material, such as wind polishing, are more commonly found near the top of the wall faces
Wall edge	Wind velocity is accelerated around the sides of objects	Acceleration can drive features such as the rounding of corners and also scouring round the base
Saltation zone	Sediment transport is concentrated within the first 40 cm above the surface	The kinetic energy of sediment laden wind can cause embedded particles to be loosened causing features such as pitting
Horizontal compaction layering	The density of earthen material is higher at the interfaces between rammed layers	Abrasional features such as pitting are concentrated on the areas of wall with lower density.
c) Rain		
Crack and joints	Faults in the earthen material can channel runoff down the wall face	Gully features are dominantly found at locations of wall weakness with depositional features such as outwash plains forming below

Once material was eroded from the parent material, wind typically entrained the earthen material, transporting it downwind, until it was either deposited in onsite dune formation or transported away from the heritage site. In contrast, material entrained in sheet or channelled runoff was typically redeposited further down the wall face or at the base of the wall (Richards et al., 2019;

Figure 6), analogous to sediment being deposited from rivers that leave mountain ranges forming alluvial fans (Bull, 1977). Consequently, products of rain-driven deterioration are likely to remain close to the parent material for longer than the products of wind-driven deterioration.

In addition to wind and rain, other environmental conditions, such as fluctuations in temperature, may impact the nature and distribution of deterioration features. At Suoyang, the low moisture content of the rammed earth (with the difference in the natural and dry density of rammed earth at Suoyang typically less than 1%; Dunhuang Academy, unpublished), suggests that deterioration mechanisms associated with processes such as freezing and ice formation are likely to be limited. However, further research is needed to assess the relative importance of these deterioration processes, especially at other earthen sites with higher moisture contents.

4.2 Magnitude and frequency of deterioration processes

Results from this study suggest that heavy rainfall events associated with dryland regions can drive the erosion of large volumes of earthen material (Table 2), but their sporadic, infrequent nature limits their overall impact (Table 3).

In contrast, individual wind events erode small volumes of earthen material but the high frequency of wind events in open, sparsely vegetated environments causes a significant cumulative impact. The cumulative impact of these low magnitude deterioration events is seen with extensive coverage of wind-driven deterioration features on walls facing the prevailing wind and also with wind controlling the location of larger features, such as turretting (Table 2). The low magnitude nature of wind as a driver of earthen deterioration means that over a recording period of days to months, these changes may not be visible and thus, further long-term studies are needed to quantify the impact of wind at earthen heritage sites.

4.3 Persistence of deterioration features

Findings from this study indicate that the persistence of deterioration at earthen heritage sites is dependent on the type of deterioration feature (Table 3). The small volume of material loss associated with the formation of wind-driven deterioration features (Figure 4 - 6) suggests many wind-driven deterioration features, such as polishing, only require small volumes of subsequent material movement to cover or erode the original feature. In addition, deterioration features, such as pitting, increase the surface area of the wall face and loosen particles from the parent material, thus increasing the area of earthen material exposed to further deterioration (Wang et al., 2010).

Conversely, the larger volumes of material movement associated with the formation of rain-driven deterioration features, such as gullies and outwash plains (Figure 6), suggest that to remove or cover over such features, greater amounts of material are subsequently required. Furthermore, the transportation and redeposition of material in solution alters the characteristics of the wall surface with the redeposited material forming a harder crust over the parent material (Cui et al., 2019). This crust can act as a protective layer as well as promoting the deterioration of the layer of material behind the crust.

The interaction between wind- and rain-driven geomorphological signatures was seen on the historic walls: rain-driven features formed over the top of wind-driven features covering the wind-driven geomorphological signature, while wind-driven features predominantly imprinted into the surface of the rain-driven feature without fully covering the underlying feature (Table 2). In cases, such as scaling off, where wind-driven deterioration caused the removal of rain-driven deterioration features, this process exposed fresh material without a geomorphological signature that could be associated with wind (Cui et al., 2019).

Given these differences in persistence, historical variations in rainfall at Suoyang could have influenced the spatial extent and severity of wind- and rain-driven geomorphological signatures. Relatively wetter periods in northwest China (e.g. 16th and mid-19th centuries) could have caused the

Deleted:

Deleted:

Deleted:

Deleted:

formation of widespread, long lasting rain-driven geomorphological signatures, while during drier periods (mid-17th to early 18th century) these signatures could have become increasingly imprinted with wind-driven deterioration features (Yang et al., 2011; Deng et al., 2017). Legacies from the wetter periods are likely to still be influencing the present-day signatures – especially if the climatic conditions caused the formation of large, highly persistent deterioration features such as turrets. Consequently, to capture: (i) the cumulative impact of low persistence, wind-driven features and (ii) the impact of potential climatic legacies, we suggest that at earthen heritage sites, geomorphological signatures have to be interpreted in conjunction with the concept of persistence.

This need for considering the concept of persistence is schematically shown in Figure 7. Figure 7 uses the findings from Suoyang to illustrate the formation and cumulative impact of wind- and rain-driven deterioration features on earthen heritage over time. The importance of the cumulative impact of wind as a driver of deterioration, presents an opportunity for earthen heritage conservation. It suggests that low-cost nature-based strategies, such as windbreaks, could be effective strategies to minimise future deterioration (Richards et al., 2020) and further research should test the efficacy of such conservation strategies at reducing deterioration at earthen heritage sites.

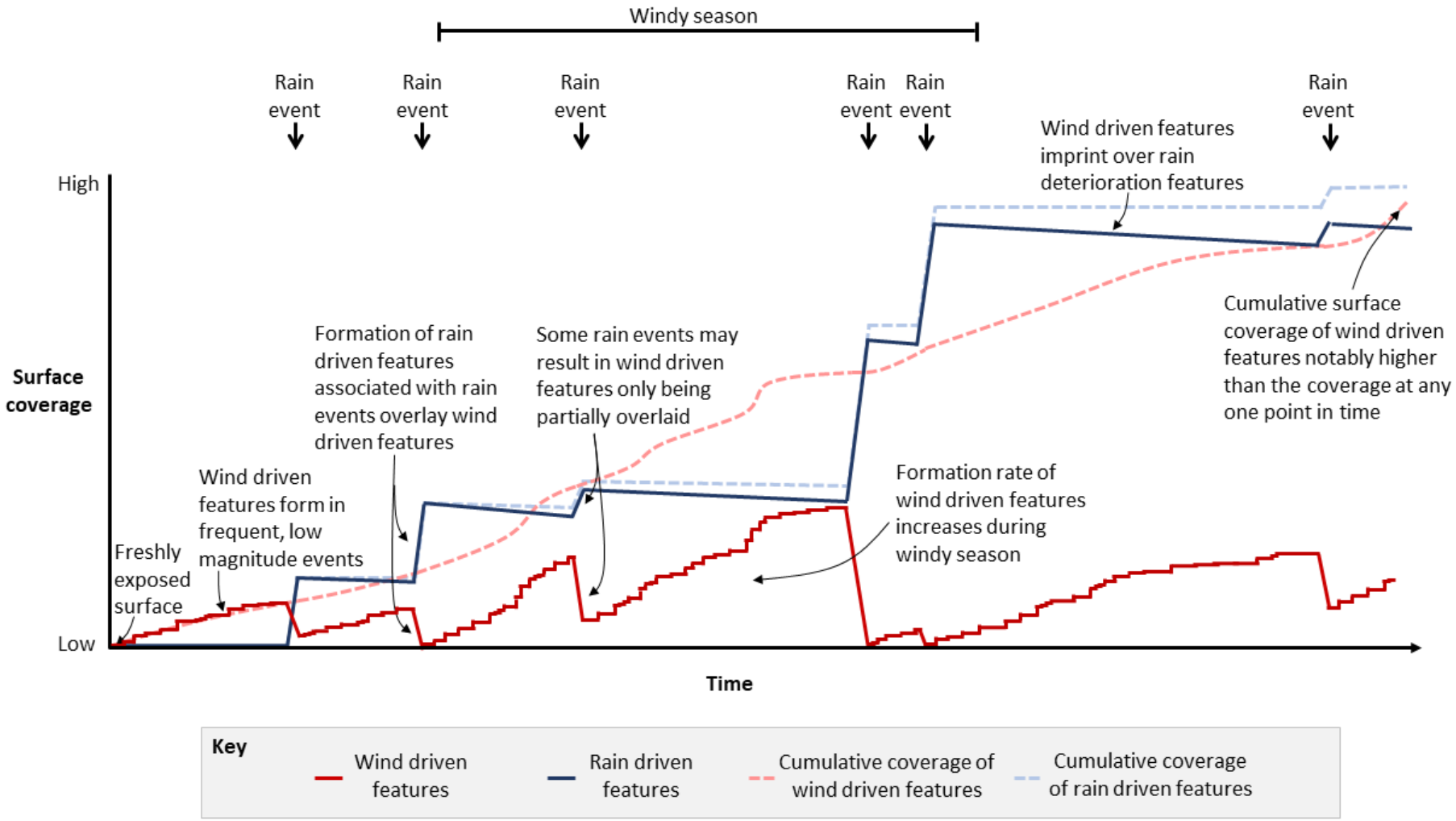

513

514 **Figure 7: A schematic of the surface coverage of wind- and rain-driven features over time. The cumulative impact of these features is shown with a dotted line.**

5 Conclusion

Many earthen heritage sites located in dryland environments are experiencing extensive deterioration. This study combined approaches from geomorphology with understandings from heritage science to investigate the relative importance of wind and rain in driving earthen heritage deterioration.

Findings from this study highlight the importance of wind as an initiator of earthen heritage deterioration, and, as a driver that can cause extensive deterioration on walls exposed to the prevailing wind.

The importance of wind is likely to have been previously overlooked due to: (i) the low magnitude of individual wind events, (ii) the small volume of material loss associated with wind-driven deterioration and (iii) the low persistence of wind-driven deterioration features. However, the cumulative effect of wind events results in wind being a vital driver of earthen heritage deterioration - with large-scale deterioration features located on walls exposed to the prevailing winds.

The outcomes from this study present an opportunity for earthen heritage conservation strategies to investigate the potential strategies that minimise wind speed at earthen heritage sites. Future research should investigate how strategies such as windbreaks could minimise future earthen deterioration as well as the deteriorative role of other environmental conditions, such as temperature fluctuations and the effects of freezing.

Conflict of interests

The authors declare no conflicts of interest.

Data Availability

Data used within this manuscript is available from the authors on request.

Author Contributions

This study was conceptualised and designed by H.V and J.R. The work was able to be undertaken with the support of Q.G. Data analysis was undertaken by J.R. with input from H.V. The writing and editing were undertaken by J.R. and H.V. All authors have read and approved the final version.

Acknowledgements

We would like to thank the two anonymous reviewers for their comments that helped improve this manuscript. We are grateful to Xudong Wang for fostering the collaboration between the Dunhuang Academy and Oxford. We are also grateful to Qiangqiang Pei for his support with this work and to Hongtao Zhan, Fei Qiu, Fasi Wu, Dongpeng He, Bo Zhang, Guojing Zhao, Jingjing Huang and Wei He for their help, advice and practical assistance they provided throughout the fieldwork period. We would like to thank Hong Zhang for all her translation work and practical assistance throughout this project. Finally, we would like to thank the Dunhuang Academy for the extensive use of their equipment in the field.

Funding: This research was funded by UK Engineering and Physical Sciences Research Council (EPSRC) grant for the Centre for Doctoral Training Science and Engineering in Art, Heritage and Archaeology (EP/L016036/1) in association with the Getty Conservation Institute. Additional funding was provided by a Royal Society International Exchange Grant (IE151144).

Data availability: Data is available from the authors on reasonable request.

References

Barton, J., 2009. 3D laser scanning and the conservation of earthen architecture: A case study at the UNESCO World Heritage Site Merv, Turkmenistan. World Archaeol. 41, 489–504. https://doi.org/10.1080/00438240903112518

Beckett, C.T.S., Jaquin, P.A., Morel, J.-C., 2020. Weathering the storm: A framework to assess the

560 resistance of earthen structures to water damage. Constr. Build. Mater. 242, 118098.
561 https://doi.org/10.1016/j.conbuildmat.2020.118098

562 Bourke, M., Brearley, J., Haas, R., Viles, H., 2007. A Photographic Atlas of Rock Breakdown Features
563 in Geomorphic Environments. Planetary Science Institute, Tuscon, Arizona, USA.

564 Bourke, M., Viles, H., Nicoli, J., Lyew-Ayee, P., Ghent, R., Holmlund, J., 2008. Innovative applications
565 of laser scanning and rapid prototype printing to rock breakdown experiments. Earth Surf.
566 Process. Landforms 33, 1614–1621. https://doi.org/10.1002/esp.1631

567 Brown, P.W., Robbins, C.R., Clifton, J.R., 1979. ADOBE II: Factors affecting the durability of adobe
568 structures. Stud. Conserv. 24, 23–39. https://doi.org/10.1179/sic.1979.003

569 Bruno, A., Bultinck, G., Chiari, G., Trossarelli, C., 1968. Contributions to the study of the preservation
570 of mud-brick structures. Mesopotamia III-IV III–IV, 445–479.

571 Brunsden, D., Thornes, J.B., 1979. Landscape sensitivity and change. Trans. Inst. Br. Geogr. 4, 403–
572 484. https://doi.org/10.2307/622210

573 Bull, W.B., 1977. The alluvial-fan environment. Prog. Phys. Geogr. Earth Environ. 1, 222–270.
574 https://doi.org/10.1177/030913337700100202

575 Crosby, A., 1983. Common sources of deterioration, in: Garrison, J.W., Ruffner, E.F. (Eds.), Adobe,
576 Practical and Technical Aspects of Adobe Conservation. Heritage Foundation of Arizona,
577 Prescott, AZ, pp. 13–18.

578 Cui, K., Du, Y., Zhang, Y., Wu, G., Yu, L., 2019. An evaluation system for the development of scaling
579 off at earthen sites in arid areas in NW China. Herit. Sci. 7, 14. https://doi.org/10.1186/s40494-
580 019-0256-z

581 Deng, Y., Gou, X., Gao, L., Yang, M., Zhang, F., 2017. Tree-ring recorded moisture variations over the
582 past millennium in the Hexi Corridor, northwest China. Environ. Earth Sci. 76, 272.

https://doi.org/10.1007/s12665-017-6581-1

Du, Y., Chen, W., Cui, K., Gong, S., Pu, T., Fu, X., 2017. A Model Characterizing Deterioration at Earthen Sites of the Ming Great Wall in Qinghai Province, China. Soil Mech. Found. Eng. 53, 426–434. https://doi.org/10.1007/s11204-017-9423-y

Du, Y., Chen, W., Cui, K., Zhang, K., 2020. Study on Damage Assessment of Earthen Sites of the Ming Great Wall in Qinghai Province Based on Fuzzy-AHP and AHP-TOPSIS. Int. J. Archit. Herit. 14, 903–916. https://doi.org/10.1080/15583058.2019.1576241

Ehlmann, B.L., Viles, H.A., Bourke, M.C., 2008. Quantitative morphologic analysis of boulder shape and surface texture to infer environmental history: A case study of rock breakdown at the Ephrata Fan, Channeled Scabland, Washington. J. Geophys. Res. Earth Surf. 113, F02012. https://doi.org/10.1029/2007JF000872

Fujii, Y., Fodde, E., Watanabe, K., Murakami, K., 2009. Digital photogrammetry for the documentation of structural damage in earthen archaeological sites: The case of Ajina Tepa, Tajikistan. Eng. Geol. 105, 124–133. https://doi.org/10.1016/J.ENGGEO.2008.11.012

Goudie, A., Stokes, S., Cook, J., Samieh, S., El-Rashidi, O.A., 1999. Yardang landforms from Kharga Oasis, south-western Egypt, in: Zeitschrift Fur Geomorphologie, Supplementband. pp. 97–112.

Goudie, A.S., Viles, H.A., 1999. The frequency and magnitude conceptin relation to rock weathering. Zeitschrift für Geomorphol. Suppl. Vol. 175–189. https://doi.org/10.1127/ZFGSUPPL/115/1999/175

Guerrero, L., 2002. Deteroriation of heritage built in adobe. Diseño y Soc. 13, 4–11.

Huinink, H.P., Pel, L., Kopinga, K., 2004. Simulating the growth of tafoni. Earth Surf. Process. Landforms 29, 1225–1233. https://doi.org/10.1002/esp.1087

Illampas, R., Ioannou, I., Charmpis, D.C., 2013. Overview of the Pathology, Repair and Strengthening

606 of Adobe Structures. Int. J. Archit. Herit. 7, 165–188.
607 https://doi.org/10.1080/15583058.2011.624254

608 Kuenen, P.H., 1948. Slumping in the Carboniferous rocks of Pembrokeshire. Q. J. Geol. Soc. London
609 104, 365–385. https://doi.org/10.1144/GSL.JGS.1948.104.01-04.18

610 Laity, J.E., 2011. Wind Erosion in Drylands, in: Arid Zone Geomorphology: Process, Form and Change
611 in Drylands. Wiley Blackwell, pp. 539–568. https://doi.org/10.1002/9780470710777.ch21

612 Laity, J.E., 2009. Landforms, landscapes, and processes of aeolian erosion, in: Parsons, A.J.,
613 Abrahams, A.D. (Eds.), Geomorphology of Desert Environments. Springer, Dordrecht,
614 Netherlands, pp. 597–627. https://doi.org/10.1007/978-1-4020-5719-919

615 Lancaster, N., 1995. Geomorphology of desert dunes. Routledge, London ; New York.

616 Lancaster, N., 1984. Characteristics and occurrence of wind erosion features in the Namib Desert.
617 Earth Surf. Process. Landforms 9, 469–478. https://doi.org/10.1002/esp.3290090507

618 Li, J., Dong, Z., Qian, G., Zhang, Z., Luo, W., Lu, J., Wang, M., 2016. Yardangs in the Qaidam Basin,
619 northwestern China: Distribution and morphology. Aeolian Res. 20, 89–99.
620 https://doi.org/10.1016/j.aeolia.2015.11.002

621 Loughlin, G.F., 1931. Notes on the weathering of natural building stones. Am. Soc. Test. Mater. 3,
622 759–767.

623 Luo, Y., Yin, B., Peng, X., Xu, Y., Zhang, L., 2019. Wind-rain erosion of Fujian Tulou Hakka Earth
624 Buildings. Sustain. Cities Soc. 50, 101666. https://doi.org/10.1016/J.SCS.2019.101666

625 Mao, X., Zhao, D., Chen, P., Hou, W., 2008. Consolidation experiment on earthen architecture site in
626 arid region. Yanshilixue Yu Gongcheng Xuebao/Chinese J. Rock Mech. Eng. 27, 7-11 [in
627 Chinese].

628 Mao, X., Zhoa, D., Zhang, W., 2015. Experimental study on the effects of wind erosion and
629 reinforcement for the rammed soil. J. Xi'an Univ. Archit. Technol. Nat. Sci. Ed. 47, 555-559 [in
630 Chinese].

631 McKay, C.P., Molaro, J.L., Marinova, M.M., 2009. High-frequency rock temperature data from hyper-
632 arid desert environments in the Atacama and the Antarctic Dry Valleys and implications for
633 rock weathering. Geomorphology 110, 182–187.
634 https://doi.org/10.1016/j.geomorph.2009.04.005

635 Messenzehl, K., Viles, H., Otto, J.-C., Ewald, A., Dikau, R., 2018. Linking rock weathering, rockwall
636 instability and rockfall supply on talus slopes in glaciated hanging valleys (Swiss Alps). Permafr.
637 Periglac. Process. 29, 135–151. https://doi.org/10.1002/ppp.1976

638 Momeni, A., Khanlari, G.R., Heidari, M., Bagheri, R., Bazvand, E., 2015. Assessment of physical
639 weathering effects on granitic ancient monuments, Hamedan, Iran. Environ. Earth Sci. 74,
640 5181–5190. https://doi.org/10.1007/s12665-015-4536-y

641 Mottershead, D.N., 2000. Identification and mapping of rock weathering surface forms and features.
642 Zeitschrift fur Geomorphol. Suppl. 120, 5–22.

643 Oliver, A., Getty Adobe Project, Getty Conservation Institute, Museum of New Mexico, 2000. Fort
644 Selden adobe test wall project: Phase I: Final report. Los Angeles, CA.

645 Peel, M.C., Finlayson, B.L., McMahon, T.A., 2007. Updated world map of the Köppen-Geiger climate
646 classification. Hydrol. Earth Syst. Sci. 11, 1633–1644. https://doi.org/10.5194/hess-11-1633-
647 2007

648 Pelletier, J.D., Kapp, P.A., Abell, J., Field, J.P., Williams, Z.C., Dorsey, R.J., 2018. Controls on Yardang
649 Development and Morphology: 1. Field Observations and Measurements at Ocotillo Wells,
650 California. J. Geophys. Res. Earth Surf. 123, 694–722. https://doi.org/10.1002/2017JF004461

651 Pu, T., Chen, W., Du, Y., Li, W., Su, N., 2016. Snowfall-related deterioration behavior of the Ming
652 Great Wall in the eastern Qinghai-Tibet Plateau. Nat. Hazards 84, 1539–1550.
653 https://doi.org/10.1007/s11069-016-2497-4

654 Richards, J., Mayaud, J., Zhan, H., Wu, F., Bailey, R., Viles, H., 2020. Modelling the risk of
655 deterioration at earthen heritage sites in drylands. Earth Surf. Process. Landforms Ahead of
656 print.

657 Richards, J., Wang, Y., Orr, S., Viles, H., Wang, Y., Orr, S.A., Viles, H., 2018. Finding Common Ground
658 between United Kingdom Based and Chinese Approaches to Earthen Heritage Conservation.
659 Sustainability 10, 3086. https://doi.org/10.3390/su10093086

660 Richards, J., Zhao, G., Zhang, H., Viles, H., 2019. A controlled field experiment to investigate the
661 deterioration of earthen heritage by wind and rain. Herit. Sci. 7, 51.
662 https://doi.org/10.1186/s40494-019-0293-7

663 Rothert, E., Eggers, T., Cassar, J., Ruedrich, J., Fitzner, B., Siegesmund, S., 2007. Stone properties and
664 weathering induced by salt crystallization of Maltese Globigerina Limestone. Geol. Soc. Spec.
665 Publ. 271, 189–198. https://doi.org/10.1144/GSL.SP.2007.271.01.19

666 Schaffer, R.J., 1932. The weathering of natural building stones. H.M. Stationery Office, London.

667 Selwitz, C., Coffman, R., Agnew, N., 1990. The getty adobe research project at Fort Selden III: An
668 evaluation of the application of chemical consolidants to test walls, in: Agnew, N. (Ed.),
669 Proceedings of the 6th International Conference on the Conservation of Earthen Architecture.
670 The Getty Institute, Los Angeles, pp. 255–260.

671 Shao, M., Li, L., Wang, S., Wang, E., Li, Z., 2013. Deterioration mechanisms of building materials of
672 Jiaohe ruins in China. J. Cult. Herit. 14, 38–44. https://doi.org/10.1016/J.CULHER.2012.03.006

673 Taylor, M.R., 1990. An evaluation of the New Mexico State monuments adobe test walls at Fort

674 Selden, in: Agnew, N. (Ed.), Proceedings of the 6th International Conference on the
675 Conservation of Earthen Architecture. The Getty Institute, Los Angeles, pp. 383–389.

676 UNESCO, 2014. Silk Roads: Initial Section of the Silk Roads, the Routes Network of Tian-shan
677 Corridor. Nomination Document.

678 Viles, H.A., 2001. Scale issues in weathering studies. Geomorphology 41, 63–72.
679 https://doi.org/10.1016/S0169-555X(01)00104-0

680 Viles, H.A., Goudie, A.S., 2013. Weathering in the central Namib Desert, Namibia: Controls, processes
681 and implications. J. Arid Environ. 93, 20–29. https://doi.org/10.1016/j.jaridenv.2011.09.012

682 Viles, H.A., Goudie, A.S., 2007. Rapid salt weathering in the coastal Namib desert: Implications for
683 landscape development. Geomorphology 85, 49–62.
684 https://doi.org/10.1016/j.geomorph.2006.03.025

685 Wang, X.D., Zhang, H.Y., Yan, G.S., Pei, Q.Q., 2010. Durability of Ancient Earthen Architecture under
686 Wind Erosion in the Milan Ancient City along the Silk Road of China. Adv. Mater. Res. 163–167,
687 3230–3236. https://doi.org/10.4028/www.scientific.net/AMR.163-167.3230

688 Ward, A.W., Greeley, R., 1984. Evolution of the yardangs at Rogers Lake, California. Bull. Geol. Soc.
689 Am. 95, 829–837. https://doi.org/10.1130/0016-7606(1984)95<829:EOTYAR>2.0.CO;2

690 WHEAP, 2012. World Heritage: Inventory of earthen architecture.

691 Wright, J.S., 2002. Geomorphology and stone conservation: Sandstone decay in Stoke-on-Trent.
692 Struct. Surv. 20, 50–61. https://doi.org/10.1108/02630800210433828

693 Xie, Y., Ward, R., Fang, C., Qiao, B., 2007. The urban system in West China: A case study along the
694 mid- section of the ancient Silk Road – He-Xi Corridor. Cities 24, 60–73.
695 https://doi.org/10.1016/j.cities.2006.11.006

696 Xu, X., Zheng, F., Wilson, G. V., Wu, M., 2017. Upslope inflow, hillslope gradient and rainfall intensity
697 impacts on ephemeral gully erosion. L. Degrad. Dev. 28, 2623–2635.
698 https://doi.org/10.1002/ldr.2825

699 Yang, B., Qin, C., Bräuning, A., Burchardt, I., Liu, J., 2011. Rainfall history for the Hexi Corridor in the
700 arid northwest China during the past 620 years derived from tree rings. Int. J. Climatol. 31,
701 1166–1176. https://doi.org/10.1002/joc.2143

702